

ANALYSIS OF TWO TIME-DELAYED SLIDING PENDULUMS

Tea Rukavina^{1,2} – Ivica Kožar^{1*}

¹Department for Computer Modeling of Materials and Structures, Faculty of Civil Engineering, University of Rijeka, Radmile Matejčić 3, 51000 Rijeka, Croatia

²Laboratoire Mécanique Roberval, Université de Technologie de Compiègne - Sorbonne Universités, Centre de Recherche Royallieu, 60205 Compiègne, France

ARTICLE INFO

Article history:

Received: 09.02.2016.

Received in revised form: 20.04.2016.

Accepted: 21.04.2016.

Keywords:

Sliding pendulums

Time delay

Elastic cable

Zipline

Abstract:

In this paper a model of two pendulums sliding along an elastic cable is presented. There is a time delay between them, so the problem has been divided into two phases in which systems of ordinary differential equations are solved. In phase one there is only one mass and the solution at the end gives the initial conditions for phase two. In phase two, the second mass is added and a system of six differential equations with six unknowns with initial conditions is derived. The validation of the model is shown in an example of a zip line structure in Croatia. Three cases are studied – when resistance is introduced when pendulums are in antiphase and when the second mass reaches the first mass.

1 Introduction

This paper is an extension of the previous work in [1] where a model of one body sliding along a cable is derived (Figure 1), and [2] where a second mass has been introduced. Here, we deal with two pendulums,

so new differential equations have to be derived, and the ones already obtained in [2] have to be modified to account for the substitution of sliding masses with sliding pendulums. This is a little more realistic representation of engineering structures such as zip

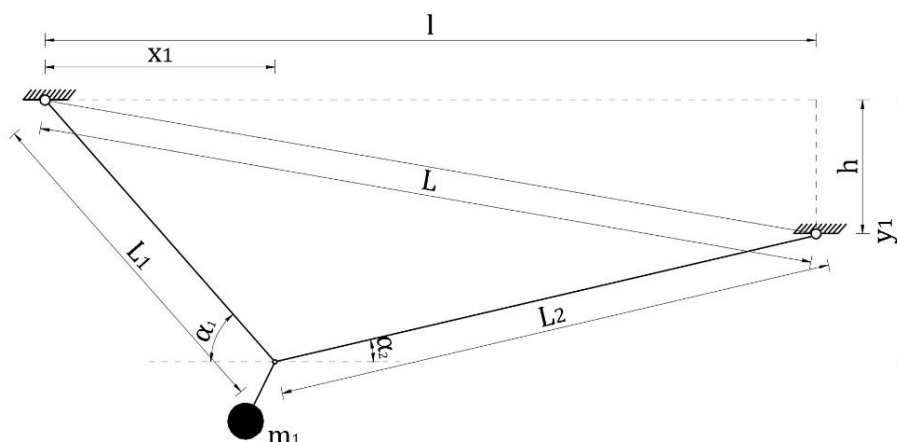


Figure 1. One pendulum sliding along a cable (phase one).

* Corresponding author. Tel.: +385 51 265 993
E-mail address: ivica.kozar@gradri.uniri.hr

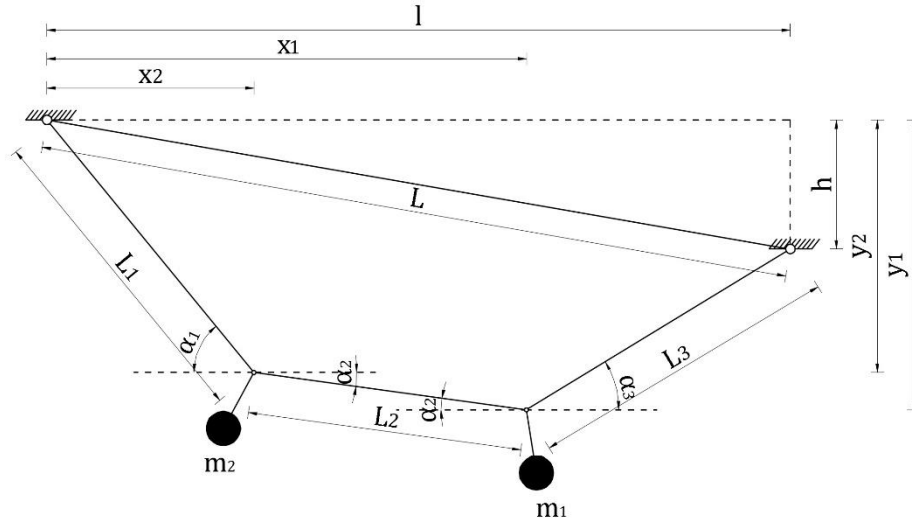


Figure 2. Two pendulums sliding along a cable (phase two).

lines, ropeways or cableways where the center of the mass is usually dislocated from the cable axis. Regarding previous works related to this topic, Brownjohn [3] describes the dynamics of a cableway system but without moving loading (masses), Bryja [4] extends the cableway analysis to a coupled moving system but without time delays and Peng [5] deals with determination of the friction coefficient between the moving cable and the pulley at a rather low speed. A possible application of the proposed model is in situations similar to the ones in [6] and [7].

2 The model

The problem of two bodies sliding along a cable with delay could be modeled by a system of Delay Differential Equation (DDEs) [8] where all terms related to the first mass depend on time t , and all terms related to the second mass depend on time $(t - \tau)$ where τ is the time delay between two pendulums. Instead of solving the DDE problem that can lead to complex computations, we have decided to simplify the calculation by dividing the problem into two phases. In phase one only the first pendulum is sliding along the cable, and in phase two the second pendulum is added. In each phase a system of ordinary differential equations (ODEs) is solved. In Figure 2, x_i denotes the horizontal, and y_i the vertical position of each mass where $i = 1$ refers to the first mass, and $i = 2$ to the second mass. A dot above a symbol denotes the derivative in time, so \dot{x}_i is the horizontal and \dot{y}_i is the vertical velocity. Two

dots stand for the second derivative of time, so \ddot{x}_i and \ddot{y}_i are the horizontal and vertical accelerations. Cable lengths are marked with L_1 , L_2 and L_3 , and l and h are the horizontal and vertical distances between the supports.

When pendulums are introduced, the mass centers are not located on the cable axis any more, but they are dislocated, so the variables x_{ip} and y_{ip} have to be introduced to define the position of the new mass centres (Figure 3):

$$\begin{aligned} x_{ip} &= x_i + L_p \sin \theta_i \\ y_{ip} &= y_i + L_p \cos \theta_i \end{aligned} \quad (1)$$

Here, L_p represents the pendulum length, which is taken to be constant for both pendulums, and θ_i is the pendulum position (angle).

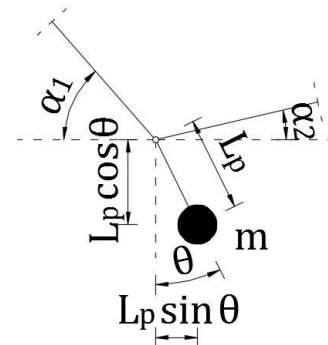


Figure 3. A pendulum.

As in [1] and [2], it is assumed that the cable is straight and its self-weight is neglected. The terms R_F and R_a that appear in the equations are used to describe resistance, and they will be explained in more detail in section 3.1.

2.1 Phase one

In phase one there is only one pendulum sliding along the cable (Figure 1). This phase ends at $t_1 = \tau$ when the second pendulum is released from the support.

The following equations have already been derived in [1], but we list them here for the sake of clarity and completeness, and because of slight changes in nomenclature.

We can start by deriving the dynamic balance equations for the first mass:

$$\begin{aligned} -T \cos \alpha_1 + T \cos \alpha_2 - R_{F1} &= m_1 \ddot{x}_{1p} \\ -T \sin \alpha_1 - T \sin \alpha_2 + m_1 g &= m_1 \ddot{y}_{1p}. \end{aligned} \quad (2)$$

An additional equation is related to the length of the cable:

$$L_1 + L_2 = L + \Delta L, \quad (3)$$

where, the elongation of the cable is defined as $\Delta L = (T L)/EA$. Here, T is the tension force, and EA is the axial stiffness of the cable.

From (3), the tension force is given/derived as:

$$T = EA \left(\frac{L_1 + L_2}{L} - 1 \right). \quad (4)$$

The equations for the lengths L_1 and L_2 and for the sines and cosines of the angles α_1 and α_2 are obtained from trigonometric relations (Figure 1):

$$\begin{aligned} L_1 &= \sqrt{x_1^2 + y_1^2}, \\ L_2 &= \sqrt{(l-x_1)^2 + (y_1-h)^2}, \\ \sin \alpha_1 &= \frac{y_1}{L_1}; \quad \cos \alpha_1 = \frac{x_1}{L_1}, \\ \sin \alpha_2 &= \frac{y_1-h}{L_2}; \quad \cos \alpha_2 = \frac{l-x_1}{L_2}. \end{aligned} \quad (5)$$

The second derivatives of the coordinates of the first mass (1) are:

$$\begin{aligned} \ddot{x}_{1p} &= \ddot{x}_1 + L_p (\ddot{\theta}_1 \cos \theta_1 - \dot{\theta}_1^2 \sin \theta_1), \\ \ddot{y}_{1p} &= \ddot{y}_1 - L_p (\ddot{\theta}_1 \sin \theta_1 + \dot{\theta}_1^2 \cos \theta_1). \end{aligned} \quad (6)$$

By inserting (4), (5) and (6) into (2), we obtain:

$$\begin{aligned} \ddot{x}_1 &= \frac{EA}{m_1} \left(\frac{L_1 + L_2}{L} - 1 \right) \left(\frac{l-x_1}{L_2} - \frac{x_1}{L_1} \right) \\ &\quad - L_p (\ddot{\theta}_1 \cos \theta_1 - \dot{\theta}_1^2 \sin \theta_1) - R_{a1}, \\ \ddot{y}_1 &= \frac{G_1}{m_1} - \frac{EA}{m_1} \left(\frac{L_1 + L_2}{L} - 1 \right) \left(\frac{y_1}{L_1} + \frac{y_1-h}{L_2} \right) \\ &\quad + L_p (\ddot{\theta}_1 \sin \theta_1 + \dot{\theta}_1^2 \cos \theta_1). \end{aligned} \quad (7)$$

From the angular balance equation

$$L_p \ddot{\theta}_1 = \ddot{y}_{1p} \sin \theta_1 - \ddot{x}_{1p} \cos \theta_1 - g \sin \theta_1, \quad (8)$$

after some transformations, we get:

$$\ddot{\theta}_1 = \frac{1}{2L_p} (\ddot{y}_1 \sin \theta_1 - \ddot{x}_1 \cos \theta_1 - g \sin \theta_1). \quad (9)$$

The initial conditions are defined as follows:

$$\begin{aligned} x_1(0) &= x_{10}, \quad \dot{x}_1(0) = 0, \quad y_1(0) = y_{10}, \\ \dot{y}_1(0) &= 0, \quad \theta_1(0) = \theta_{10}, \quad \dot{\theta}_1(0) = 0. \end{aligned} \quad (10)$$

The initial horizontal position x_{10} and the initial angle θ_{10} can be chosen at will. The initial value for y_{10} is obtained from Equation:

$$G_1 - EA \left(\frac{L_1 + L_2}{L} - 1 \right) \left(\frac{y_1}{L_1} + \frac{y_1-h}{L_2} \right) = 0. \quad (11)$$

Equations (7) and (9), with initial conditions (10), form a system of three differential equations with three unknowns. As it was explained in [2], the values for $x_1, \dot{x}_1, y_1, \dot{y}_1, \theta_1$ and $\dot{\theta}_1$ at the end of this phase are the initial conditions for the first mass in phase two,

and they are named $x_{1\tau}, \dot{x}_{1\tau}, y_{1\tau}, \dot{y}_{1\tau}, \theta_{1\tau}$ and $\dot{\theta}_{1\tau}$, respectively.

2.2 Phase two

Phase two begins when the second pendulum is released from the support, while the first pendulum continues to slide (Figure 2). Time t_2 starts at τ . Again, we can start with the dynamic balance equations for both masses [2]:

$$\begin{aligned} -T \cos \alpha_2 + T \cos \alpha_3 - R_{F1} &= m_1 \ddot{x}_{1p}, \\ -T \sin \alpha_2 - T \sin \alpha_3 + m_1 g &= m_1 \ddot{y}_{1p}, \\ -T \cos \alpha_1 + T \cos \alpha_2 - R_{F2} &= m_2 \ddot{x}_{2p}, \\ -T \sin \alpha_1 - T \sin \alpha_2 + m_2 g &= m_2 \ddot{y}_{2p}. \end{aligned} \quad (12)$$

Equation (3) now takes the form:

$$L_1 + L_2 + L_3 = L + \Delta L, \quad (13)$$

so the tension force is:

$$T = EA \left(\frac{L_1 + L_2 + L_3}{L} - 1 \right). \quad (14)$$

The lengths and the sines and cosines are again defined from trigonometric relations (Figure 2):

$$\begin{aligned} L_1 &= \sqrt{x_2^2 + y_2^2} \\ L_2 &= \sqrt{(x_1 - x_2)^2 + (y_1 - y_2)^2} \\ L_3 &= \sqrt{(l - x_1)^2 + (y_1 - h)^2} \\ \sin \alpha_1 &= \frac{y_2}{L_1}; \quad \cos \alpha_1 = \frac{x_2}{L_1} \\ \sin \alpha_2 &= \frac{y_1 - y_2}{L_2}; \quad \cos \alpha_2 = \frac{x_1 - x_2}{L_2} \\ \sin \alpha_3 &= \frac{y_1 - h}{L_2}; \quad \cos \alpha_3 = \frac{l - x_1}{L_2} \end{aligned} \quad (15)$$

The coordinates of the second mass are defined by:

$$\begin{aligned} x_{2p} &= x_2 + L_p \sin \theta_2, \\ y_{2p} &= y_2 + L_p \cos \theta_2, \end{aligned} \quad (16)$$

and their second derivatives are:

$$\begin{aligned} \ddot{x}_{2p} &= \ddot{x}_2 + L_p (\ddot{\theta}_2 \cos \theta_2 - \dot{\theta}_2^2 \sin \theta_2), \\ \ddot{y}_{2p} &= \ddot{y}_2 - L_p (\ddot{\theta}_2 \sin \theta_2 + \dot{\theta}_2^2 \cos \theta_2). \end{aligned} \quad (17)$$

An additional angular equation has to be introduced:

$$\ddot{\theta}_2 = \frac{1}{2L_p} (\ddot{y}_2 \sin \theta_2 - \ddot{x}_2 \cos \theta_2 - g \sin \theta_2). \quad (18)$$

By substituting (6), (9), (14), (15), (17) and (18) into (12), after some transformations, a system of six equations with six unknowns is obtained:

$$\begin{aligned} \ddot{x}_1 &= \frac{EA}{m_1} \left(\frac{L_1 + L_2 + L_3}{L} - 1 \right) \left(\frac{l - x_1}{L_3} - \frac{x_1 - x_2}{L_2} \right) - \\ &\quad - L_p (\ddot{\theta}_1 \cos \theta_1 - \dot{\theta}_1^2 \sin \theta_1) - R_{a1}, \\ \ddot{y}_1 &= \frac{G_1}{m_1} - \frac{EA}{m_1} \left(\frac{L_1 + L_2 + L_3}{L} - 1 \right) \left(\frac{y_1 - y_2}{L_2} + \right. \\ &\quad \left. + \frac{y_1 - h}{L_3} \right) + L_p (\ddot{\theta}_1 \sin \theta_1 + \dot{\theta}_1^2 \cos \theta_1), \\ \ddot{\theta}_1 &= \frac{1}{2L_p} (\ddot{y}_1 \sin \theta_1 - \ddot{x}_1 \cos \theta_1 - g \sin \theta_1), \\ \ddot{x}_2 &= \frac{EA}{m_2} \left(\frac{L_1 + L_2 + L_3}{L} - 1 \right) \left(\frac{x_1 - x_2}{L_2} - \frac{x_2}{L_1} \right) - \\ &\quad - L_p (\ddot{\theta}_2 \cos \theta_2 - \dot{\theta}_2^2 \sin \theta_2) - R_{a2}, \\ \ddot{y}_2 &= \frac{G_2}{m_2} + \frac{EA}{m_2} \left(\frac{L_1 + L_2 + L_3}{L} - 1 \right) \left(\frac{y_1 - y_2}{L_2} - \right. \\ &\quad \left. - \frac{y_2}{L_1} \right) + L_p (\ddot{\theta}_2 \sin \theta_2 + \dot{\theta}_2^2 \cos \theta_2), \\ \ddot{\theta}_2 &= \frac{1}{2L_p} (\ddot{y}_2 \sin \theta_2 - \ddot{x}_2 \cos \theta_2 - g \sin \theta_2). \end{aligned} \quad (19)$$

In phase two, the initial conditions for the first mass are the final results obtained from phase one. The initial conditions for the second mass are the same as the ones already derived in [2], but we have to

introduce four new conditions for θ_1 , $\dot{\theta}_1$, θ_2 and $\dot{\theta}_2$. All the initial conditions for phase two are listed here:

$$\begin{aligned} x_1(\tau) &= x_{1\tau}, & \dot{x}_1(\tau) &= \dot{x}_{1\tau}, & y_1(\tau) &= y_{1\tau}, \\ \dot{y}_1(\tau) &= \dot{y}_{1\tau}, & \theta_1(\tau) &= \theta_{1\tau}, & \dot{\theta}_1(\tau) &= \dot{\theta}_{1\tau}, \\ x_2(\tau) &= x_{2\tau}, & \dot{x}_2(\tau) &= 0, & y_2(\tau) &= y_{2\tau}, \\ \dot{y}_2(\tau) &= 0, & \theta_2(\tau) &= \theta_{2\tau}, & \dot{\theta}_2(\tau) &= 0. \end{aligned} \quad (20)$$

The terms $x_{2\tau}$ and $\theta_{2\tau}$ can be chosen at will, and $y_{2\tau}$ is obtained from Equation:

$$G_2 + EA \left(\frac{L_1 + L_2 + L_3}{L} - 1 \right) \left(\frac{y_1 - y_2}{L_2} - \frac{y_2}{L_1} \right) = 0. \quad (21)$$

Now the model is completely defined.

3 Example

The same example is taken as in [1] and [2], and the geometric and material properties correspond to a real engineering structure – a zip line – in Omiš, Croatia:

$$\begin{aligned} l &= 600.0 \text{ m}, \\ h &= 60.0 \text{ m}, \\ L &= 603.2 \text{ m}, \\ EA &= 6 \cdot 10^6 \text{ N}, \\ L_p &= 1.0 \text{ m}, \\ m_1 &= m_2 = 150.0 \text{ kg}. \end{aligned} \quad (22)$$

This example is solved using Wolfram Mathematica [10]. Mathematica can solve systems of differential equations symbolically using the function `DSolve` and numerically using the function `NDSolve`. `DSolve` has more restrictions on the system to be solved, so a numerical solution has been applied in the paper. The default setting in `NDSolve` for the integration procedure is “Automatic” when the internal algorithm chooses between the fixed and adaptive step size, explicit or implicit procedure etc. The user can override the “Automatic” setting, and during numerical testing several options have been tried out, all with the same results and comparable execution times. Even the simplest integration procedure has been tried out, for instance, the “Linearly Implicit Euler” with “Fixed step”, with the same result for the system of 6 differential equations but significantly longer solution time. The conclusion is that the choice of the numerical integration

procedure is not significant for the problem presented in this paper.

The analysis time in phase one is taken to be $t_{1,max} = \tau = 10 \text{ s}$. The analysis time in phase two is taken to be $t_{2,max} = 15 \text{ s}$. This is slightly before the first mass reaches the support on the right side, because it is not desirable that the first mass reflects back from the support. So, the total analysis time is $t_{max} = t_{1,max} + t_{2,max} = 25 \text{ s}$. For now, it is assumed that there is no resistance, so $R_{a1} = R_{a2} = 0$.

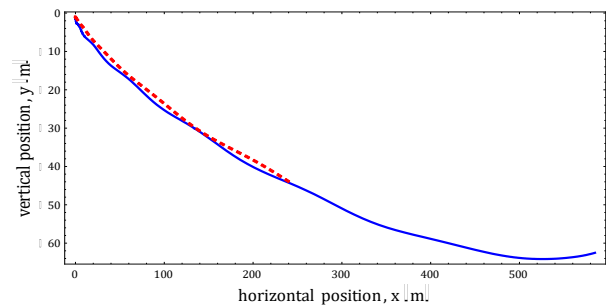


Figure 4. The path of the first mass (blue solid) and second mass (red dashed).

In Figure 4, the paths of the masses in both phases are shown where the solid blue line represents the path of the first mass and the dashed red line the path of the second mass. In the total analysis time t_{max} , the first mass has almost reached the support $(x_1, y_1) = (585.1 \text{ m}; 61.5 \text{ m})$, and mass two has reached the point $(x_2, y_2) = (234.3 \text{ m}; 43.4 \text{ m})$.

Figure 5 shows the horizontal velocities of both masses in time, and Figure 6 shows their vertical velocities.

The maximum velocities for the first mass are: $\dot{x}_{1,max} = 35.4 \text{ m/s}$, and $\dot{y}_{1,max} = 4.2 \text{ m/s}$, and for the second mass: $\dot{x}_{2,max} = 28.7 \text{ m/s}$, and $\dot{y}_{2,max} = 4.3 \text{ m/s}$. The tension force in the cable is shown in Figure 7.

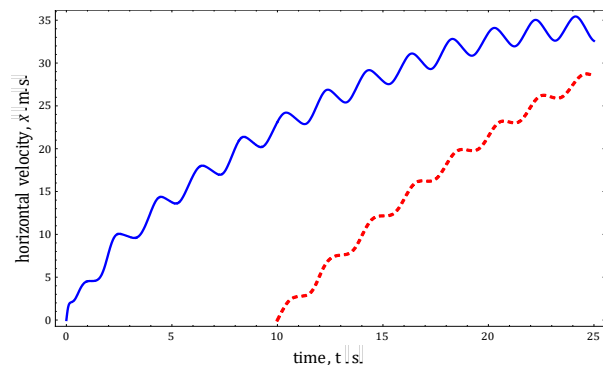


Figure 5. Horizontal velocity of the first mass (blue solid) and second mass (red dashed).

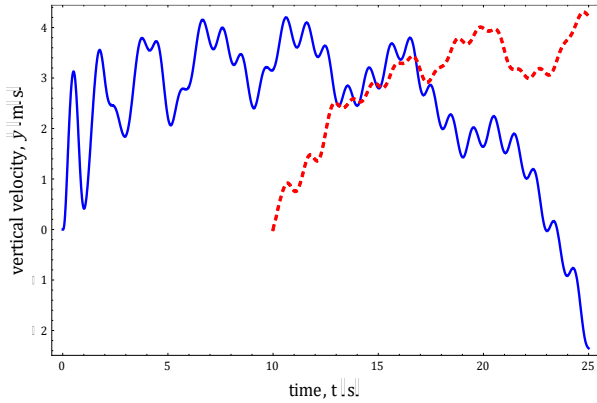


Figure 6. Vertical velocity of the first mass (blue solid) and second mass (red dashed).

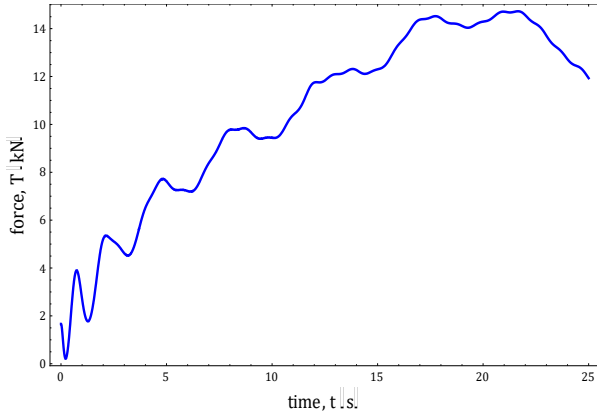


Figure 7. Tension force in the cable.

Figure 8 shows that pendulum angles for the first and second mass range from -0.76 to 0.40 radians. It can be noticed that both pendulums are swaying in phase if the initial pendulum angles for both masses are chosen to be zero.

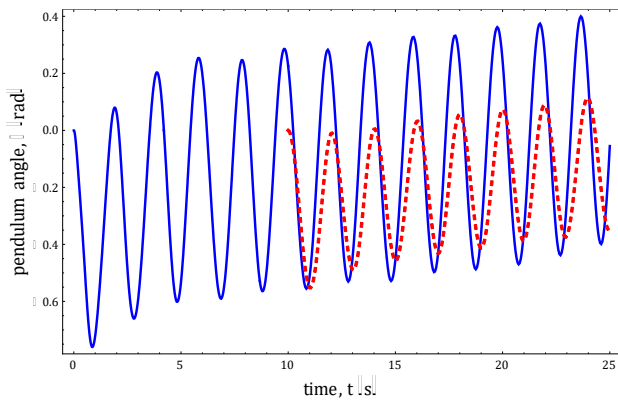


Figure 8. Pendulum angle for the first mass (blue solid) and second mass (red dashed).

3.1 Introduction of resistance

Resistance R is intended for the approximate assessment of motion resistant forces like braking, friction, wind resistance etc., but without describing each of them in detail since their equations differ significantly [5], [9].

The braking force is realized through a braking moment resulting in a jump in the cable's internal forces. The introduction of friction and braking force would change the cable force T into $(T + R)$ before the pendulum and $(T - R)$ after the pendulum. In this case, R would appear in both equations, for horizontal and for vertical force balance (2). Aerodynamic (wind) resistant force is [9]:

$$F = \int p \, dA = \frac{1}{2} \rho v^2 \int C_p \, dA, \quad (23)$$

where, ρ and v are the mass and velocity of the fluid and C_p is a dimensionless coefficient. The force acts on the pendulum mass and would appear in (7).

Both resistance forces are difficult to predict: the duration and intensity of braking is user controlled and wind resistance depends on the coefficient C_p that is shape and velocity dependent. Authors have decided that resistant forces should be approximately taken into account through a function that could only reduce the velocity of the pendulum and stop it before the end of the cable (as it happens in reality).

The braking (friction) resistance type is described in (2) where R has the dimension of force with the term $-R (\cos \alpha_1 + \cos \alpha_2)$ for the horizontal force balance and $R (\sin \alpha_1 - \sin \alpha_2)$ for the vertical force balance. Since R is not known, cosines in the first term are assumed to be one, and the sine difference is assumed to be zero. As a result, the resistance force R_F appears only in the first equation.

The wind resistance type is described in (19) and this is what has been calculated in numerical experiments. In (19), R_a has the dimension of acceleration since $R_a = R_{wind} / m_{pendulum}$. The exact force R_{wind} is not known but it is, namely, approximated so that the pendulum stops before end of the cable. The simplest procedure that can be carried out through trial and error is the use of the logistic function (Figure 9) for direct approximation of R_a as a function of the horizontal position. More realistically, R_a should be a function of velocity, but that would require a separate numerical procedure just for the determination of R_a .

The logistic function shows that initial exponential growth is followed by a period in which growth slows and then levels off, approaching (but never attaining) a maximum upper limit [11].

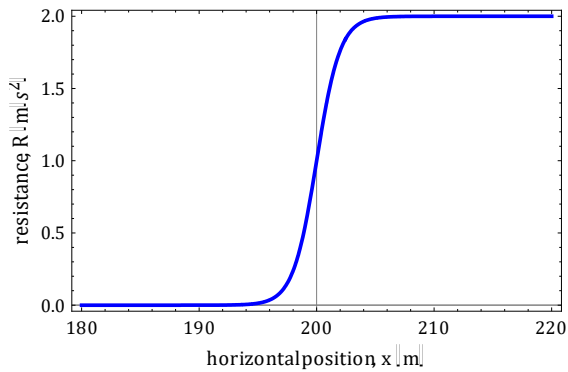


Figure 9. Logistic function.

The logistic function is described with the following equation:

$$R_a = \frac{R_{a,max}}{1 + e^{-k(x-x_m)}} \quad (24)$$

where, $R_{a,max}$ is the maximum value of resistance, k is the steepness of the curve, and x_m is the midpoint. The chosen parameter values in this example are $R_{a,max} = 2 \text{ m/s}^2$, $k = 1$, $x_m = 200 \text{ m}$.

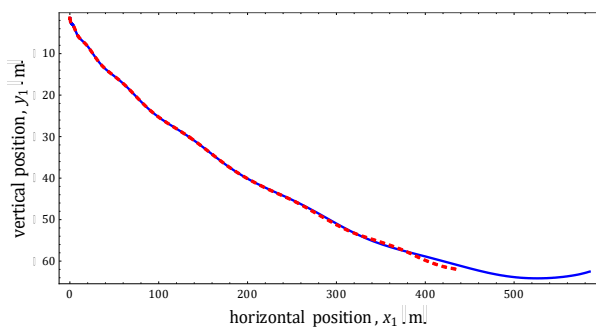


Figure 10. The path of the first mass – without resistance (blue solid) and with resistance (red dashed).

In Figures 10-13, the path, velocity and pendulum angle for the first mass are shown, the values of which/whose values are compared for the case with and without resistance. From Figure 10 it can be seen that the first mass does not come so near the support any more, but only reaches $x_1 = 438.3 \text{ m}$.

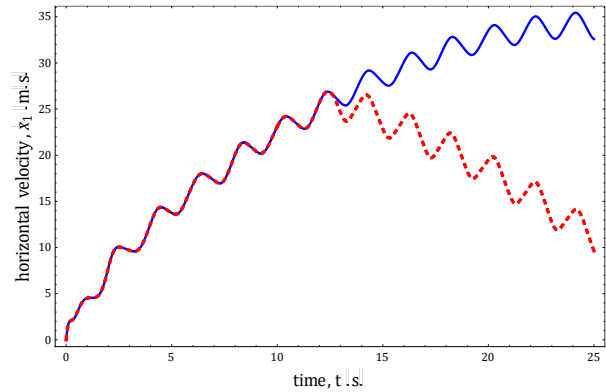


Figure 11. Horizontal velocity of the first mass – without resistance (blue solid) and with resistance (red dashed).

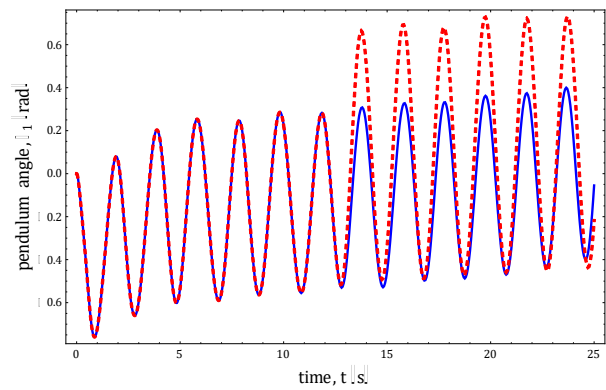


Figure 12. Pendulum angle for the first mass – without resistance (blue solid) and with resistance (red dashed).

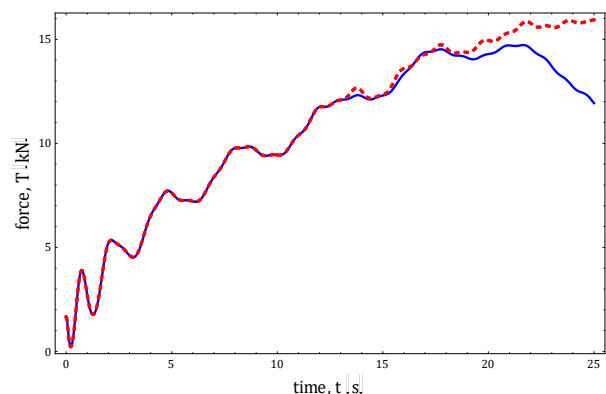


Figure 13. Tension force in the cable – without resistance (blue solid) and with resistance (red dashed).

It can be seen that the resistance starts acting around time $t = 13 \text{ s}$ when the velocity starts to decrease (Figure 11), and the pendulum angle increases

(Figure 12). Also, the tension force in the cable increases because of it (Figure 13).

3.2 Pendulums in antiphase

In the first example when initial pendulum angles were zero for both masses, it was shown that pendulums were swaying in phase (Figure 8). Is there any difference when the pendulums are in antiphase (Figure 14)?

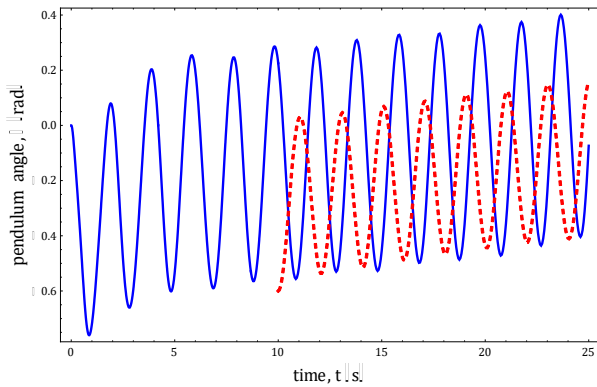


Figure 14. Pendulum angle for the first mass (blue solid) and the second mass (red dashed) when they are in antiphase.

In this case, the mass paths do not change significantly, and the major differences are found in the horizontal and vertical velocity of the second mass (Figures 15 and 16).

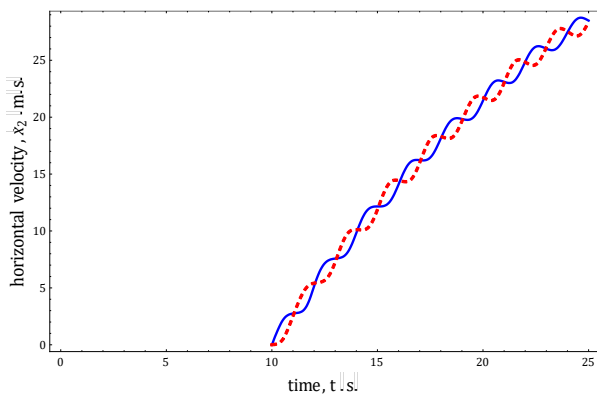


Figure 15. Horizontal velocity of the second mass – pendulums in phase (blue solid) and in antiphase (red dashed).

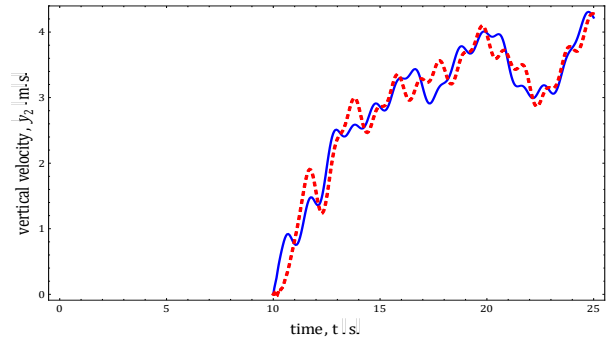


Figure 16. Vertical velocity of the second mass – pendulums in phase (blue solid) and in antiphase (red dashed).

3.3 Catching up

It is interesting to observe what happens if the second mass reaches the first mass. For example, this can be accomplished by shortening the time interval τ between the two masses, or by giving the second mass an initial speed. Here, both ways were used, so the second mass is released from the support at $t_{1,max} = \tau = 5$ s, and an initial speed $\dot{x}_2(\tau) = 10$ m/s has been given to the second mass. To have the same total analysis time as in the previous examples ($t_{max} = 25$ s), the duration of phase two has to be $t_{2,max} = 20$ s.

It has been calculated that the second mass catches up with the first mass at $t = 19$ s. In this model, no conditions for the impact have been introduced, and the behavior of the masses is shown in the following figures.

When the masses come near each other, the velocity of the first mass is increased (Figure 17), and the velocity of the second mass decreased (Figure 18). Also, the collision makes the pendulums sway in opposite directions, increasing their amplitudes (Figure 19).

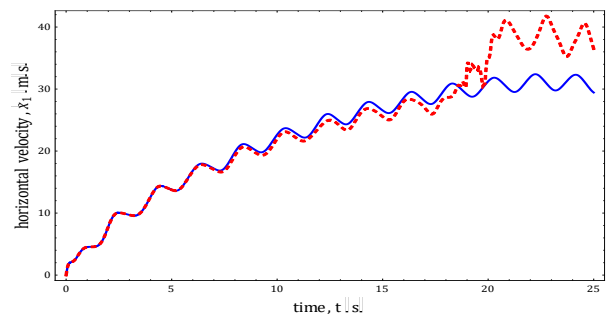


Figure 17. Horizontal velocity of the first – without initial speed of the second mass (blue solid) and with initial speed of the second mass (red dashed).

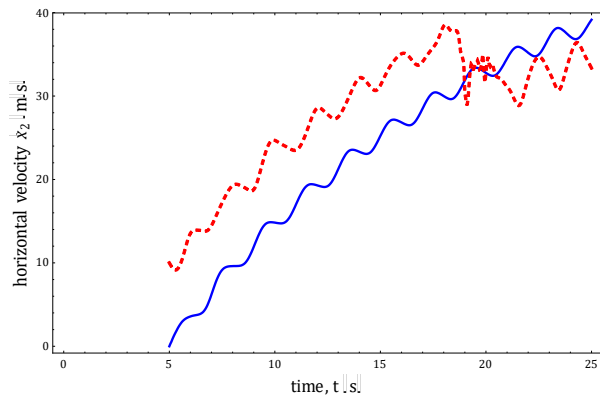


Figure 18. Horizontal velocity of the second mass – without initial speed of the second mass (blue solid) and with initial speed of the second mass (red dashed).

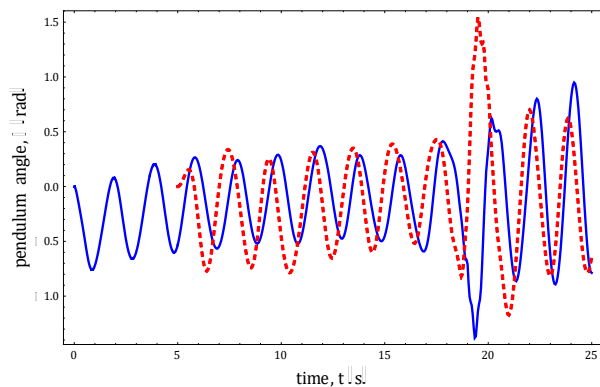


Figure 19. Pendulum angle for both masses with initial speed of the second mass – first mass (blue solid) and second mass (red dashed).

This model could be developed further, i.e. by introducing a condition that the two masses connect in the moment when they come near, so they continue sliding along the cable together. Also, in order to consider the friction, in a future extension of this paper, the velocity dependent resistance force could be developed.

4 Conclusion

The model of pendulums sliding along a cable is a coupled problem, because a cable imposes nonlinear constraints onto dynamic equations of mass movement [1]. This leads to a differential algebraic system of equations that can be solved using various solvers, e.g. Wolfram Mathematica. The example

solved in this paper has proven the validity of the model and some special cases have been analyzed – with resistance force, with pendulums in antiphase, and the case where the second mass reaches the first. It has been shown that this problem can be modeled as a non-linear system of differential equations, in analytical form, without the need for finite element discretization.

References

- [1] Kožar, I., Torić Malić, N.: *Analysis of body sliding along cable*, Coupled Systems Mechanics, 3 (2014), 3, 291-304.
- [2] Rukavina, T., Kožar, I.: *Analysis of two masses sliding along a cable with delay*, Proceedings of the International Conference on Applied Mathematics and Computational Methods in Engineering (AMCME 2015), Barcelona, Spain, 2015, 61-64.
- [3] Brownjohn, J. M. W.: *Dynamics of an aerial cableway system*, Engineering Structures, 20 (1998), 9, 826-836.
- [4] Bryja, D., Knawa, M.: *Computational model of an inclined aerial ropeway and numerical method for analyzing nonlinear cable-car interaction*, Computers and Structures, 89 (2011), 21-22, 1895-1905.
- [5] Peng, Y., Zhu, Z., Chen, G., Cao, G.: *Effect of tension on friction coefficient between lining and wire rope with low speed sliding*, Journal of China University of Mining and Technology, 17 (2007), 3, 409-413.
- [6] Ivić, S., Čanadžija, M., Družeta, S.: *Static structural analysis of S-lay pipe laying with a tensioner model based on the frictional contact*, Engineering Review, 34 (2014), 3, 223-234.
- [7] Petranović, D., Marušić, A.: *Application of genetic algorithms in wire busbars design with 3D truss portals*, Engineering Review, 35 (2015), 3, 309-316.
- [8] Shampine, L. F., Gladwell, I., Thompson, S.: *Solving ODEs with Matlab*, Cambridge University Press, New York, 2003.
- [9] Houghton, E. L., Carruthers, N. B.: *Wind forces on buildings and structures: an introduction*, Edward Arnold Publishers Ltd., London, 1976.
- [10] Wolfram Language and System, Documentation Center, 2015, <http://reference.wolfram.com/language/>.
- [11] Finan, M. B.: *A reform approach to business calculus*, Arkansas Tech University, 2003, <http://faculty.atu.edu/mfinan/bcalbook.pdf>.